Regular Article

PHYSICAL CHEMISTRY RESEARCH
Published by the
Iranian Chemical Society
www.physchemres.org
info@physchemres.org

Phys. Chem. Res., Vol. 10, No. 3, 333-344, September 2022
DOI: 10.22036/PCR.2021.304087.1966

Experimental and Theoretical Spectroscopic Studies of the Electronic Structure of 2-Ethyl-2-phenylmalonamide

S. Selvaraj[a,*], A. Ram Kumar[b], T. Ahilan[c], M. Kesavan[d], G. Serdaroglu[e], P. Rajkumar[f], M. Mani[g], S. Gunasekaran[h] and S. Kumaresan[g]

[a]*Department of Science and Humanities, St. Joseph College of Engineering, Sriperumbudur, Chennai-602117, Tamil Nadu, India*
[b]*PG and Research Department of Biochemistry, Indo-American College, Cheyyar-604407, Tamil Nadu, India*
[c]*Department of Mechanical Engineering, St. Joseph's College of Engineering, Sriperumbudur, Chennai-602117, Tamil Nadu, India*
[d]*Interdisciplinary Institute of Indian System of Medicine, SRM Institute of Science and Technology, Kattankulathur, Chennai -603203, Tamil Nadu, India*
[e]*Faculty of Education, Mathematics and Science Education, Sivas Cumhuriyet University, Sivas 58040, Turkey*
[f]*PG and Research Department of Physics, King Nandhivarman College of Arts and Science, Thellar-604406, Affiliated to Thiruvalluvar University, Serkkadu, Vellore-632 115, Tamil Nadu, India*
[g]*Spectrophysics Research Laboratory, PG and Research Department of Physics, Arignar Anna Government Arts College, Cheyyar-604407, Tamil Nadu, India*
[h]*Sophisticated Analytical Instrumentation Facility, St. Peter's Institute of Higher Education and Research, St. Peter's University, Avadi, Chennai-600054, Tamil Nadu, India*
(Received 10 September 2021, Accepted 1 December 2021)

The present study aimed to provide a deeper understanding of the structure and spectroscopic properties of 2-ethyl-2-phenylmalonamide. To this end, the optimized geometrical parameters, vibrational wavenumbers, and electronic spectra of 2-ethyl-2-phenylmalonamide were calculated theoretically using density functional theory (DFT)/B3LYP with the 6-311++G(d,p) basis set. The experimental vibrational wavenumbers were calculated by Fourier transform-infrared (FT-IR) and Fourier transform Raman (FT-Raman) spectra recorded in the region of 4000-400 cm^{-1}. The ^{1}H and ^{13}C nuclear magnetic resonance (NMR) chemical shifts were calculated using the gauge-independent atomic orbital (GIAO) method. The gas-phase UV-Vis spectrum was recorded and compared with the theoretical spectrum. Other molecular properties, such as natural bond orbital (NBO) analysis, were also carried out to determine stability and charge delocalization. In addition, the molecular electrostatic potential surface was stimulated to study the electrophilic and nucleophilic sites of the title compound. The theoretically calculated values showed good agreement with the observed spectra, confirming the structure of 2-ethyl-2-phenylmalonamide.

Keywords: 2-Ethyl-2-phenylmalonamide, DFT, Vibration spectra, FT-IR, FT-Raman, NMR

INTRODUCTION

As a common neurological disorder, an epileptic seizure is found in both males and females, affects the central nervous system, and is characterized by abnormal cortical activity in the brain [1,2]. In 2019, World Health Organization (WHO) estimated that about 50 million people worldwide were affected by epilepsy. Brain injury, tumors, infections (*e.g.*, meningitis), mutations in and thus the upregulation of the mTOR pathway, and high levels of sodium and glucose have been reported to cause epileptic seizures [3-5]. Anticonvulsant drugs, also known as

*Corresponding author. E-mail: sselvaphy@gmail.com

antiepileptic drugs, are used to treat epileptic seizures [6]. Antiepileptic drugs, such as valproic acid, phenytoin, and carbamazepine, can reduce or eliminate seizures in the majority of patients. However, these medicines are associated with undesirable side effects, such as weight gain and hepatotoxicity [7-8]. 2-Ethyl-2-phenylmalonamide (2E2PM), also known as phenylethylmalonamide, with a molecular formula of $C_{11}H_{14}N_2O_2$, a molecular weight of 206.24 g mol^{-1}, two hydrogen donors, one acceptor, and four rotatable bonds, is a primary active metabolite of primidone [9]. The chemical structure of 2E2PM differs from that of primidone due to the ring cleavage. From the structural point of view, 2E2PM contains a phenyl ring and an ethyl group linked to malonamide. As an active and abundant metabolite in humans, phenylethylmalonamide is derived naturally from the ethanolic seed extract of *Abrus precatorius* (L) and chemically from 2-hydroxypyrimidine, which is prepared by alkaline hydrolysis and converted to phenylethylmalonamide with the help of primidone, a hepatic microsomal enzyme inducer [10-12]. While no significant pharmaceutical activity has been reported for phenylethylmalonamide, some studies have reported the use of phenylethylmalonamide in the treatment of essential tremor and epileptic seizures [13]. Some other studies have attempted to determine and analyze the concentration of phenylethylmalonamide in plasma and urine samples of humans using gas chromatography [14]. A study reported that phenylethylmalonamide enhanced the anticonvulsant activity of phenobarbital and the hypnotic activity of hexobarbital [15]. Moreover, phenylethylmalonamide and primidone were found in lake water with a concentration of 0.6 μg l^{-1} and 0.2 μg l^{-1}, respectively [16].

DFT is an effective tool to predict molecular structures and vibrational wavenumbers of biologically active compounds and drug molecules. The literature review revealed that there had been no detailed theoretical and experimental spectroscopic studies on the structure of phenylethylmalonamide. Accordingly, the present study investigated the structural and vibrational properties of phenylethylmalonamide using theoretical (DFT) and experimental (FT-IR, FT-Raman, ^{1}H and ^{13}C NMR, and UV-Vis spectra) methods to provide a better understanding of the electronic, structural, and spectroscopic properties of phenylethylmalonamide.

MATERIALS AND METHODS

Experimental

2E2PM was obtained from Sigma-Aldrich Chemical Co (St. Louis, MO, USA) in powder form and with 98% purity. 2E2PM is used for spectral measurements without any modifications. The FT-IR spectrum of the titled compound was recorded in the region of 4000-400 cm^{-1} using Perkin-Elmer Spectrum Two FTIR/ATR Spectrometer system with 0.5 cm^{-1} resolution. The FT-Raman was also recorded in the same region on a Bruker RFS 27 Stand alone FT-Raman Spectrometer system with 2 cm^{-1} resolution using the 1064 nm line of Nd:YAG laser with 100 mW power as an excitation source. The ^{1}H and ^{13}C NMR spectra were recorded in dimethyl sulfoxide (DMSO) solution and methanol on a Bruker high-resolution NMR spectrometer at 300 K. The chemical shifts were expressed in ppm relative to internal tetramethylsilane (TMS) standard. The ultraviolet-visible (UV-Vis) spectrum was measured in the wavelength range of 200-400 nm using a Perkin-Elmer Lambda 35 UV Winlab V6.0 Spectrometer with a bandwidth of 0.5-4 nm at room temperature.

Computational Details

The quantum chemical calculations were performed for 2E2PM using Gaussian 09 W program with 6-311++G(d,p) as the basis set to determine its optimized geometry and vibrational wavenumbers at the DFT/B3LYP level of theory [17-20]. The vibrational assignments were made using the Chemcraft program [21], which provided a graphic visualization with a high degree of accuracy. The ^{1}H and ^{13}C NMR chemical shifts were calculated in the gas phase by the gauge-including atomic orbital (GIAO) method using B3LYP with the 6-311++G(d,p) basis set. GIAO is one of the most common methods used to calculate nuclear magnetic shielding tensors and determine molecular geometries and magnetic properties [22-23]. The UV-Vis spectra and electronic properties of 2E2PM were determined by time-dependent density functional theory (TD-DFT) method at the B3LYP/6-311++G(d,p) level of theory [24-25]. NBO analysis of 2E2PM was performed using B3LYP with the 6-311++G(d,p) basis set. The molecular electrostatic potential surface was plotted using ArgusLab software [26].

RESULTS AND DISCUSSION

Optimized Geometry

The optimized molecular structure of 2E2PM with atomic numbering is shown in Fig. 1. The geometrical parameters, such as bond lengths and bond angles, were theoretically calculated by DFT/B3LYP/6-311++G(d,p). Since the crystal structure of 2E2PM was not available in the literature as yet, an attempt was made to use the values closely related to the 2-phenylmalonamide structure [27]. The calculated and experimental values of bond lengths and bond angles of 2E2PM are presented in Table S1 (Supplementary material).

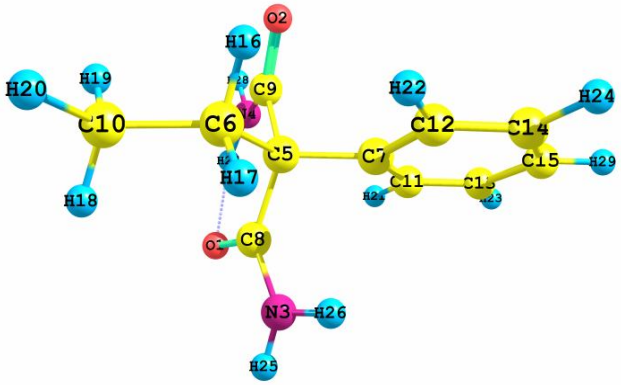

Fig. 1. The optimized molecular structure of 2-ethyl-2-phenylmalonamide.

From the literature review, C=C and C-C bond lengths were expected to fall in the range of 1.35 and 1.45 Å [28,29]. The optimized bond lengths of C=C and C-C were calculated theoretically in the range of 1.395-1.403 Å and 1.391-1.569 Å and experimentally at 1.386-1.391 Å and 1.376-1.384 Å, respectively. The bond lengths of C_5-C_6, C_5-C_7, C_5-C_8, C_5-C_9, and C_6-C_{10} had values higher than the expected range, which can be attributed to the influence of oxygen and nitrogen ions on the carbonyl and amine groups tending to attract electrons to themselves. Due to the regular hexagonal structure of the benzene ring, the bond angles around the carbon atom are expected to be 120° [29]. The C-C-C bond angles were experimentally observed in the range of 110.2-121.4° and theoretically calculated in the range of 105.5-123°. The title compound, which has two carbonyl groups (C=O) attached to carbon (C_5), is expected to be in the range of 1.22 Å [30]. Based on the geometrical properties, the bond length of C=O was theoretically calculated in the range of 1.220-1.226 Å and experimentally observed in the range of 1.231-1.237 Å whereas the C-O-H and O-C-C bond angles were theoretically calculated in the range of 103.0° and 118.5-124.8°, respectively, and experimentally observed at 118.8-121.6°. The values obtained showed good agreement with those reported in the literature.

The bond length of the intramolecular hydrogen bonding was theoretically calculated at 1.875 Å. The intramolecular charge transfer between the amine and the carbonyl group suggested the formation of a new partial bond between hydrogen and oxygen. The bond length of C-H was theoretically calculated in the range of 1.082-1.093 Å and experimentally observed at 0.952-1.017 Å whereas the C-C-H and H-C-H bond angles were theoretically calculated in the range of 106.8-120.5° and 107.5-107.9°, respectively, and experimentally observed at 118.6-121.6°. The optimized bond lengths of N-H and N-C were theoretically calculated in the range of 1.008-1.015 Å and 1.353-1.360 Å and experimentally observed at 0.853-0.950 Å and 1.321-1.324 Å, respectively. The bond angles of O-C-N, H-N-H, C-N-H, and N-C-C were theoretically calculated in the range of 120.6-123.4°, 118.5-120.8°, 116.6-121.2°, and 114.4-118.1°, respectively, which were in agreement with the experimental data observed at 122.5-123.2°, 120.2-120.3, 117.8-121.7°, and 115.9-118.0°, respectively. The theoretically optimized values were in good coincidence with the experimental values, with a linear coefficient value (R_2) of 0.98194 for bond lengths and 0.44112 for bond angles. The correlation graph between the experimental and theoretical values is shown in Fig. S1 (Supplementary material).

Vibrational Spectral Analysis

2E2PM consists of 29 atoms, 81 normal modes of vibrations, and (3N-6) vibration degrees of freedom. From C_1 point group symmetry, the vibration of the title compound is distributed as 14 stretching vibrations, 31 in-plane bending vibrations, and 36 out-of-plane bending vibrations. The theoretical and experimental spectra are shown in Figs. 2 and 3, and the complete theoretical and

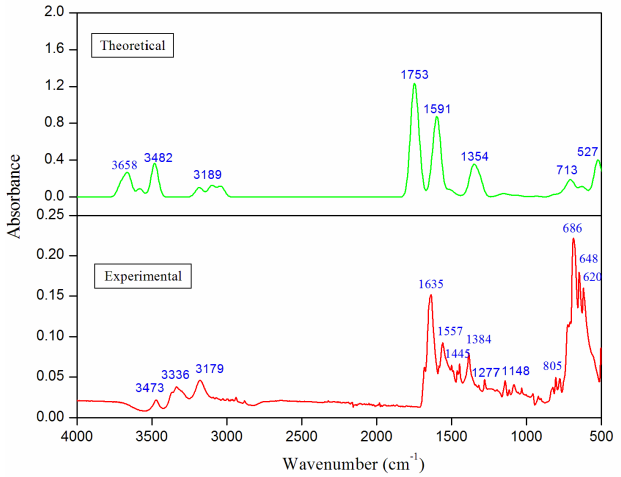

Fig. 2. The theoretical and experimental FT-IR spectra of 2-ethyl-2-phenylmalonamide.

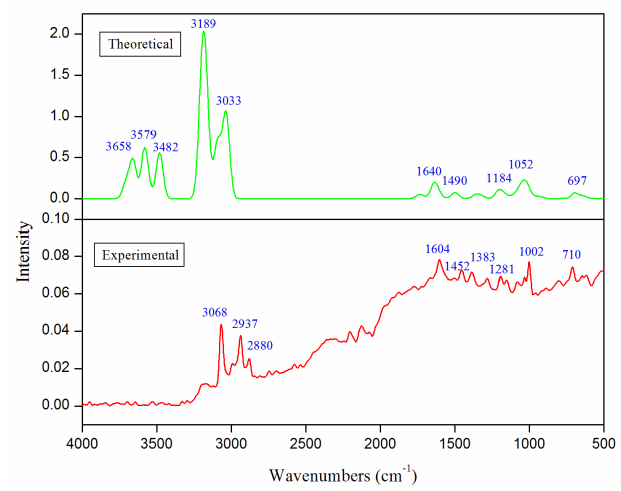

Fig. 3. The theoretical and experimental FT-Raman spectra of 2-ethyl-2-phenylmalonamide.

experimental wavenumbers are presented in Table S2 (Supplementary material). Based on the results, it can be said that 2E2PM has six characteristic bands (*i.e.*, CC, CH_2, CH_3, CH, CO, and NH_2) in the functional group region and bending vibrations in the fingerprint region. The experimental results were compared with the theoretical calculations obtained by DFT/B3LYP with the 6-311++G(d,p) basis set. The characteristic spectral vibrations are discussed below. The calculated vibrational frequencies were obtained by a scaling factor of 0.96 for all frequencies.

NH_2 Vibrations

The title compound contained two NH_2 groups. Hence, one can expect it to have two symmetric and asymmetric vibrations. In general, NH_2 symmetric and asymmetric stretching vibrations appear in the range of 3450-3250 cm^{-1} and 3550-3330 cm^{-1}, respectively [31]. In the present study, the asymmetric stretching modes were calculated at 3557-3152 cm^{-1}, respectively, and experimentally observed at 3473 cm^{-1} in the FT-IR spectrum with a deviation of 39 cm^{-1} due to the intermolecular hydrogen bonding between the amino group and the carbonyl group. The symmetric stretching vibrations were experimentally observed at 3336 cm^{-1} in the FT-IR spectrum and theoretically calculated at 3436-3343 cm^{-1}. The bending vibrations of NH_2, such as scissoring, rocking, wagging, and twisting, were observed in the region of 1630-1610, 1090-1060, 700-500, and below 500 cm^{-1} [32]. Based on the above literature, scissoring vibrations of NH_2 were calculated theoretically at 1683, 1654, 1574, 1555, 1552, and 1527 cm^{-1} and assigned experimentally at 1557 cm^{-1} in the FT-IR and at 1604 cm^{-1} in the FT-Raman spectrum. NH_2 rocking vibrations were observed at 1105, 1081, 1060, and 1053 cm^{-1}, showing good agreement with the experimental FT-IR spectrum at 1084 cm^{-1} and the FT-Raman spectrum at 1080 cm^{-1}. The wagging vibrations were observed and assigned at 777, 648, 620, and 503 cm^{-1} in the FT-IR spectrum and at 617 cm^{-1} in the FT-Raman spectrum, and the corresponding theoretical values were calculated at 741, 731, 669, 658, 614, 548, and 506 cm^{-1}. The twisting vibrations of NH_2 were calculated theoretically at 440, 338, and 373 cm^{-1} and observed experimentally at 442 cm^{-1} in the FT-Raman spectrum.

CH Vibrations

The CH stretching vibrations usually appear in the range of 3100-3000 cm^{-1} [33,34]. In the present investigation, the CH stretching vibrations were calculated theoretically at 3076, 3061, 3050, 3040, 3033, and 2972 cm^{-1} and observed experimentally at 3179 cm^{-1} in the FT-IR spectrum and at 3068 cm^{-1} in the FT-Raman spectrum. The in-plane and out-of-plane bending vibrations appear at 1530-1000 cm^{-1} and 1000-750 cm^{-1}, respectively [35,36]. Based on the results, CH in-plane bending vibrations of 2E2PM showed three bands at 1557, 1148, and 1084 cm^{-1} in the FT-IR spectrum

and six bands at 1452, 1192, 1152, 1080, 1031, and 1002 cm^{-1} in the FT-Raman spectrum whereas the theoretically calculated bands were in the range of 1574-1010 cm^{-1}. The CH out-of-plane bending vibrations were calculated theoretically at 976-741 cm^{-1} and observed experimentally at 777 cm^{-1} in the FT-IR spectrum.

CH_3 Vibrations

The title compound contains a single methyl group and electron-donating substitutions in the aromatic ring system. One can expect nine fundamental vibrations, such as symmetric stretching, asymmetric stretching, symmetric deformation, asymmetric deformation, in-plane rocking, out-of-plane rocking, twisting mode, and wagging mode, in the methyl group. The symmetric and asymmetric methyl group stretching vibrations are generally observed in the range of 2870 and 2980 cm^{-1} [37]. In this study, the asymmetric vibrations were calculated theoretically at 2972, 2965, and 2912 cm^{-1}, which showed good agreement with the experimental FT-Raman spectrum at 2880 cm^{-1}. The asymmetric and symmetric bending vibrations are expected to fall in the range of 1465-1440 and 1390-1370 cm^{-1}, respectively [38]. The CH_3 asymmetric bending vibrations of the title compound were calculated theoretically at 1464, 1444, and 1441 cm^{-1}, which showed excellent correlation with the experimental FT-IR spectrum at 1445 cm^{-1} and the FT-Raman spectrum at 1452 cm^{-1}. The CH_3 symmetric bending vibrations were calculated theoretically at 1365 cm^{-1}, which showed good agreement with the experimental FT-IR and FT-Raman spectra at 1384 and 1383 cm^{-1}, respectively.

CH_2 Vibrations

The CH_2 group shows six fundamental frequencies, including symmetric, asymmetric, two in-plane bending vibrations (*i.e.*, scissoring and rocking), and two out-of-plane bending vibrations (*i.e.*, wagging and twisting). The symmetric and asymmetric stretching vibrations are observed at 3000-2900 and 3100-3000 cm^{-1}, respectively [39]. In the present study, the calculated wavenumbers observed at 2986, 2965, 2924, and 2912 cm^{-1} were assigned to asymmetric stretching vibrations and observed experimentally at 2937 cm^{-1} in the FT-Raman spectrum. The bending vibrations were observed in the region below 1500 cm^{-1} [40]. Based on the results, the CH_2 scissoring modes were calculated theoretically at 1441, 1430, 1416, and 1365 cm^{-1}, and a single band was observed at 1384 and 1383 cm^{-1} in the experimental FT-IR and FT-Raman spectra. The bands at 1277 and 1281 cm^{-1} in the FT-IR and FT-Raman spectra, respectively, corresponded to the experimental CH_2 wagging vibration and were calculated theoretically at 1316, 1271, 1269, 924, and 888 cm^{-1}. The CH_2 twisting vibrations were calculated theoretically at 1256, 1122, 1105, 1081, 926, and 881 cm^{-1}, and a single band was observed at 1084 in the experimental FT-Raman spectrum and at 1080 cm^{-1} in the FT-IR spectrum. The rocking vibrations of CH_2 were calculated theoretically at 780, 741, and 589 cm^{-1} and observed experimentally at 805 and 777 cm^{-1} in the FT-IR spectrum and at 799 cm^{-1} in the FT-Raman spectrum, respectively. The theoretical wavenumbers showed a good correlation with the experimental observations.

CC and C=O Vibrations

The CC stretching vibrations are very prominent and highly characteristic in aromatic rings and usually appear in the range of 1650-1200 cm^{-1} [41]. From the theoretical calculation, five bands were observed at 1654, 1574, 1555, 1269, and 1256 cm^{-1}, and a single band was observed experimentally at 1557 cm^{-1} in the FT-IR spectrum. The carbonyl group is very sensitive to physical and chemical factors. The C=O stretching vibrations are expected to fall in the range of 1850-1550 cm^{-1} [42]. In the present study, the C=O stretching vibrations were calculated theoretically at 1683-1654 cm^{-1} and observed experimentally at 1635 in the FT-IR spectrum and at 1604 cm^{-1} in the FT-Raman spectrum, respectively. In the theoretical and experimental FT-IR, the broadband was observed at 1683 and 1635 cm^{-1} due to a protonated carbonyl group.

CN Vibrations

It is very difficult to evaluate the CN vibration due to the mixing of several bands in the same region. While the frequencies of the C=N group are expected to be around 1500 cm^{-1}, frequencies around 1300 cm^{-1} indicate the presence of C-N for aromatic compounds [43-45]. In a study, a band at 1310 cm^{-1} was observed in the FT-Raman spectrum as the CN stretching mode [46]. In the present

investigation, these bands were observed experimentally at 1277 cm^{-1} in the FT-IR spectrum and at 1281 cm^{-1} in the FT-Raman spectrum and calculated theoretically at 1271-1256 cm^{-1}.

Chemical Shifts

NMR is a common technique used to determine the molecular structure and magnetic properties of chemical compounds [47]. The theoretically calculated and experimentally observed spectra of ^{13}C and ^{1}H NMR for 2E2PM are presented in Table 1. The experimental ^{1}H and ^{13}C NMR spectra of 2E2PM are shown in Figs. 4, 5, 6, and 7. In organic compounds, carbon atoms are observed in the range of 150-100 ppm and hydrogen atoms in the range of 8.00-7.00 ppm [48-50]. The title compound contains eleven carbon atoms, six carbons (C_3, C_7, C_8, C_9, C_{10}, and C_{11}) in the benzene ring structure, one carbon in the methyl group, one in the methylene group, two carbons attached to oxygen atoms, and one carbon linked to the ring structure. In this study, the carbon atoms (C_3, C_7, C_8, C_9, C_{10}, and C_{11}) in the benzene ring structure were observed experimentally at 127.34-141.99 ppm in DMSO and at 128.85-142.63 ppm in methanol and calculated theoretically in the range of 130.04-143.01 ppm. Carbon atom C_6 in the methyl group, shielded by protons, showed an upfield region of the spectrum observed experimentally at 10.34 ppm in DMSO and at 10.73 ppm in methanol and calculated theoretically at 11.38 ppm. Carbon atoms C_4 and C_5, surrounded by two adjacent electronegative atoms and with more deshielded shifts, were observed experimentally at 174.67 in DMSO and at 178.13 in methanol and calculated theoretically at 176 ppm. The carbon atom C_2 in the CH_2 group was more shielded at 37.94 ppm in DFT and at 27-29 ppm in experimental chemical shifts.

The chemical shift of hydrogen atoms, attached to carbon atoms in the benzene rings (H_6, H_7, H_8, H_9, and H_{14}), was observed experimentally at 7.32-7.99 ppm in DMSO and at 7.35-7.39 pm in methanol and calculated theoretically at 7.44-7.89 ppm. The methyl group protons (H_3, H_4, and H_5) were experimentally observed at 0.82-0.85 ppm in DMSO and at 0.92-0.95 ppm in methanol as a triplet and theoretically calculated at 0.98-1.22 ppm. The hydrogen atom in the methylene group (H_1, H_2) was observed experimentally at 2.31-2.30 ppm in DMSO and at 2.35-2.34 ppm in methanol and calculated theoretically in the range of 2.08 and 2.12 ppm. The hydrogen atoms (H_{10}, H_{11}, H_{12}, and H_{13}) in amino groups were observed at 7.23-7.31 ppm in DMSO and at 7.23-7.29 ppm in methanol and calculated theoretically at 4.17-4.32 ppm due to the influence of nitrogen atoms. The theoretically optimized values were in good coincidence with the experimental values with a linear coefficient value (R_2) of 0.99797 for DMSO and 0.99738 for methanol. The correlation graph between experimental and theoretical values is shown in Fig. S2 (Supplementary material).

Table 1. Experimental and Theoretical ^{1}H and ^{13}C NMR Chemical Shifts of 2-Ethyl-2-phenylmalonamide

Atoms	Theoretical	Experimental	
	B3LYP/6-311++ G(d,p)	DMSO	Methanol
H_1	2.126	2.313	2.354
H_2	2.086	2.300	2.340
H_3	1.219	0.857	0.953
H_4	1.228	0.843	0.938
H_5	0.981	0.829	0.924
H_6	7.877	7.998	7.389
H_7	7.673	7.386	7.385
H_8	7.441	7.361	7.357
H_9	7.517	7.344	7.389
H_{10}	4.313	7.311	7.299
H_{11}	4.099	7.261	7.269
H_{12}	4.170	7.248	7.235
H_{13}	4.322	7.236	7.233
H_{14}	7.439	7.326	7.392
C_1	63.12	61.81	63.59
C_2	37.94	27.93	29.98
C_3	143.01	141.99	142.63
C_4	176.29	174.67	178.13
C_5	176.14	174.67	178.13
C_6	11.38	10.34	10.73
C_7	130.04	127.42	130.21
C_8	123.72	127.34	129.24
C_9	136.92	128.60	128.85
C_{10}	136.70	128.60	128.85
C_{11}	132.72	128.60	128.85

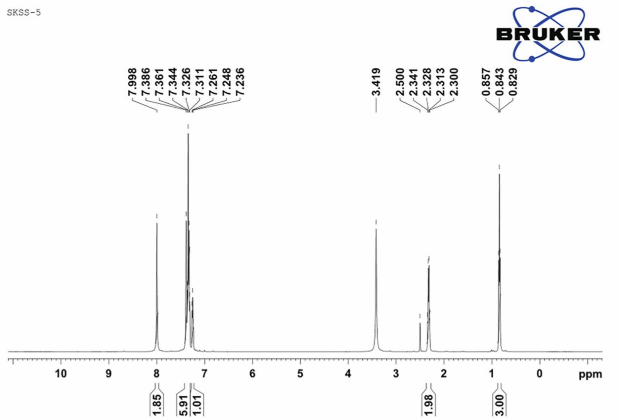

Fig. 4. The experimental ^{1}H NMR spectrum of 2-ethyl-2-phenylmalonamide in DMSO.

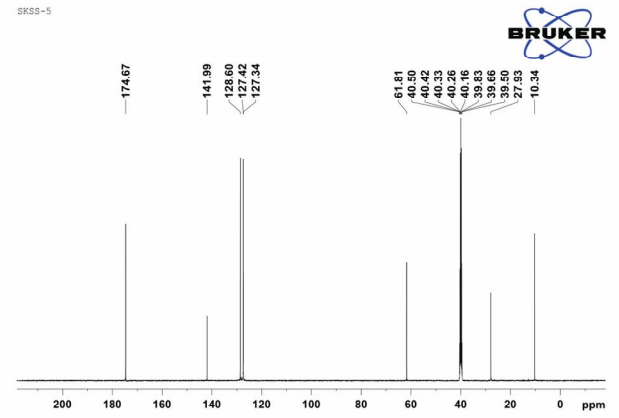

Fig. 5. The experimental ^{13}C NMR spectrum of 2-ethyl-2-phenylmalonamide in DMSO.

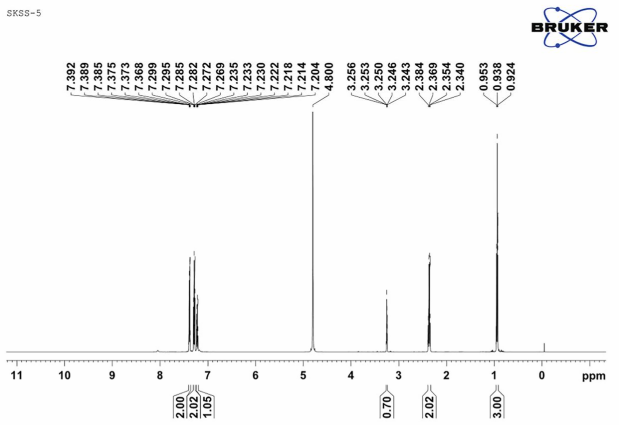

Fig. 6. The experimental ^{1}H NMR spectrum of 2-ethyl-2-phenylmalonamide in methanol.

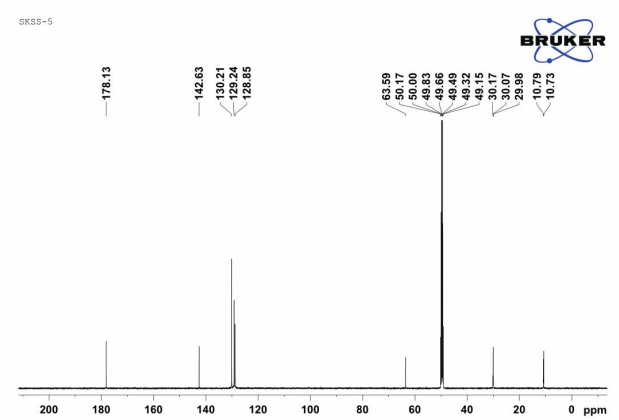

Fig. 7. The experimental ^{13}C NMR spectrum of 2-ethyl-2-phenylmalonamide in methanol.

Table 2. Experimental and Calculated Wavelengths (λ), Excitation Energies (E), Absorbance Values, Oscillator Strengths (f), and Major Contributions of 2-Ethyl-2-Phenylmalonamide

Experimental		TDDFT/B3LYP/6-311++G(d,p)			
λ (nm)	Abs	λ (nm)	E (eV)	F	Major contributions
-	-	270	4.5793	0.0109	HOMO→LUMO (75%)
259	0.1107	259	4.7755	0.0329	HOMO→LUMO+1 (75%)
225	1.0112	253	4.8917	0.0018	HOMO→LUMO+6 (54%)

Electronic Properties

The theoretical electronic spectrum of 2E2PM was calculated by TD-DFT calculations with B3LYP/6-311++G(d,p) level of theory. Furthermore, the experimental electronic spectrum was measured in ethanol solvent, and the results were compared with those of the theoretical spectrum. The theoretical absorption, wavelength (λ), excitation energies (E), oscillator strength (f), experimental absorption, and wavelength (λ) are presented in Table 2, and the corresponding spectra are shown in Figs. 8 and 9. From the experimental analysis, one sharp band was obtained at 225 nm and one weak band at 259 nm, and the

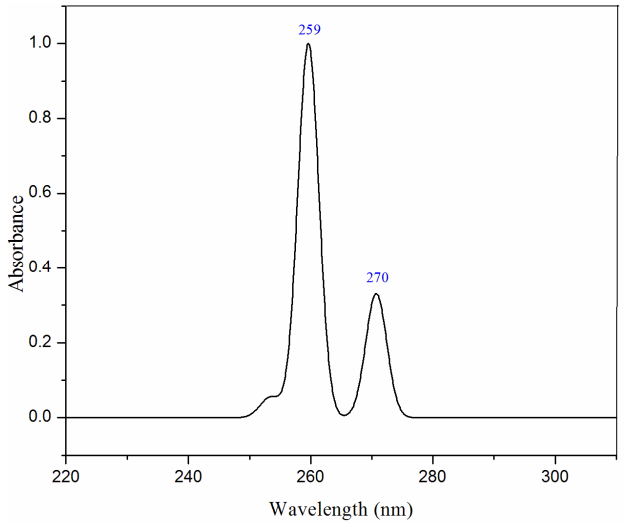

Fig. 8. The theoretical electronic spectrum of 2-ethyl-2-phenylmalonamide.

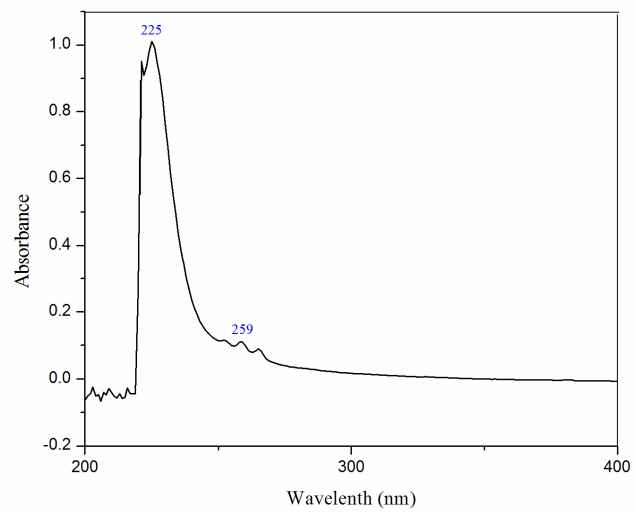

Fig. 9. The experimental electronic spectrum of 2-ethyl-2-phenylmalonamide.

corresponding theoretical spectra were calculated at 259.63 and 253.46 nm. The theoretical and experimental results were nearly close to each other and showed a good correlation.

NBO Analysis

The second-order perturbation energy analysis based on the NBO analysis was introduced by Weinhold and colleagues [51-55] to describe the non-covalency, H-bonding, and conjugative interactions, *etc*. For a specific system, the second-order perturbation energy lowering of the donor (i) → acceptor (j) interaction is defined as follows:

$$E^{(2)} = \Delta E_{ij} = q_i \frac{(F_{ij})^2}{(\varepsilon_j - \varepsilon_i)}$$

where $E^{(2)}$ is the donor-acceptor stabilization energy, qi is the donor orbital occupancy, εi and εj are donor and acceptor orbital energies (diagonal elements), and Fij is the off-diagonal NBO Fock matrix element.

Due to their importance in the biomedical and related scientific disciplines, intramolecular interactions for different kinds of molecular systems have been reported in previous studies [56-58] to explore/evaluate conjugative interactions. In this work, the NBO study of the 2E2PM was performed, and the results of the second-order perturbation energy analysis are presented in Table S3. As expected from previous reports [59-60], the biggest contribution to $E^{(2)}$ was due to the charge movement from the lone pair of the nitrogen to the unoccupied molecular orbital energies. The $E^{(2)}$ for both interactions, namely, LP (1) N_3(ED_i = 1.76175e) → π* C_1-O_8 (ED_j = 0.24879e) and LP (1) N_4 (ED_i = 1.76186e) → π* C_1-O_8 (ED_j = 0.24879e), was determined by the energy of 55.12 kcal mol^{-1}. Moreover, the electron movement on the unsaturated ring of the 2E2PM had an essential role in lowering the energy. The interactions on the unsaturated ring were estimated as π C_7-C_{12}→ π* C_{11}-C_{13}($E^{(2)}$ = 18.94 kcal mol^{-1}), π C_7-C_{12}→ π* C_{14}-C_{15} ($E^{(2)}$ = 20.02 kcal mol^{-1}), π C_{11}-C_{13}→ π* C_7-C_{12} ($E^{(2)}$ = 25.65 kcal mol^{-1}), π C_{11}-C_{13}→ π* C_{14}-C_{15} ($E^{(2)}$ = 20.21 kcal mol^{-1}), π C_{14}-C_{15}→ π* C_7-C_{12} ($E^{(2)}$ = 18.30 kcal mol^{-1}), and π C_{14}-C_{15}→ π* C_{11}-C_{13} ($E^{(2)}$ = 20.46 kcal mol^{-1}). It should be noted that these interactions were responsible for changing the polarity on the molecular surface and thus affecting the chemical reactivity.

Molecular Electrostatic Potential Surface

The molecular electrostatic potential of 2E2PM is illustrated in Fig. S3 (Supplementary material) and was used to determine its molecular structure and physiochemical properties. In molecular electrostatic potential surface, the

values are represented by different colors, and the potential increases in the order of red < orange < yellow < green < blue [61]. Red color indicates more negativity, the preferred site for electrophilic attack, and strongest repulsion whereas blue color indicates the strongest attraction site for nucleophilic attack. From the results, it was clear that oxygen had a significant red color, indicating that electronegativity is an electron-rich site. Blue also indicates positive charges around hydrogen atoms. The intensity of the color is directly proportional to the potential energy.

CONCLUSIONS

In this study, the optimized molecular geometry, vibrational wavenumbers, and magnetic properties of 2E2PM were recorded and analyzed for the first time. The calculated optimized geometrical parameters showed good agreement with the experimental data. The experimental FT-IR and FT-Raman spectra were done and compared with the recorded theoretical wavenumbers. The results were promising and showed a good correlation between experimental and calculated normal modes of vibration. The chemical shifts of ^{13}C and ^{1}H NMR were calculated theoretically and compared with the experimental values. The results showed that carbon atom C_2 had a more shielded signal at 37.94 ppm in theoretical and at 27 and 29 ppm in experimental chemical shifts. The gas-phase UV-Vis spectrum was also recorded by TD-DFT, and the values were in good agreement with the experimental values. In addition, NBO confirmed that the strongest intramolecular interaction was 55.12 kcal mol^{-1} *via* LP N_3 and N_4 to π^* O_1-C_8. The charge distribution and electric potential on the surface were determined by molecular electrostatic potential surface. The detailed experimental and theoretical findings were in good agreement, confirming the structure of the title compound.

ACKNOWLEDGEMENTS

The authors would like to thank SAIF, St. Peters University, Chennai, Tamil Nadu, India, for recording the FT-IR and UV-Vis spectral measurements. The authors are also thankful to SAIF, IIT Madras, Chennai, for recording the FT-Raman spectral measurements, and CSIF, IIISM, SRM University, Chennai, for recording the NMR spectral measurements.

REFERENCES

[1] Fauser, S.; Tumani, H., *Chapter 15-Epilepsy: Handbook of Clinical Neurology*. Elsevier B.V: **2017**, *146 (3rd series)*; pp. 259-266, DOI: 10.1016/B978-0-12-804279-3.00015-0.

[2] Shoeibi, A.; Ghassemi, N.; Alizadehsani, R.; Rouhani, M.; Hosseini-Nejad, H.; Khosravi, A.; Panahiazar, M.; Nahavandi, S., A comprehensive comparison of handcrafted features and convolutional autoencoders for epileptic seizures detection in EEG signals. *Expert Syst. Appl*. **2021**, *163*, 113788, DOI: 10.1016/j.eswa.2020.113788.

[3] Leonetti, A.; Baroli, G.; Fratini, E.; Pietropaoli, S.; Marcoli, M.; Mariottini, P.; Cervelli, M., Epileptic seizures and oxidative stress in a mouse model over-expressing spermine Oxidase. *Amino Acids*. **2020**, *52*, 129-139, DOI: 10.1007/s00726-019-02749-8.

[4] Manford, M., Recent advances in epilepsy, *J. Neurol*. **2017**, *264*, 1811-1824, DOI: 10.1007/s00415-017-8394-2.

[5] Orsini, A.; Zara, F.; Striano, P., Recent advances in epilepsy genetics. *Neurosci. Lett*. **2018**, *667*, 4-9, DOI: 10.1016/j.neulet.2017.05.014.

[6] Cotterman-Hart, S., *Chapter 11 - Antiepileptic drugs: First generation: Epilepsy and Brain Tumors*. Elsevier B.V: **2015**, pp. 159-169, DOI: 10.1016/B978-0-12-417043-8.00011-0.

[7] Zhang, T.; Yu, F.; Xu, H.; Chen, M.; Chen, X.; Guo, L.; Zhou, C.; Xu, Y.; Wang, F.; Yu, J.; Wu, B., Dysregulation of REV-ERBα impairs GABAergic function and promotes epileptic seizures in preclinical models. *Nat. Commun*. **2021**, *12*, 1-14, DOI: 10.1038/s41467-021-21477-w.

[8] Youssef, F. S.; Menze, E. T.; Ashour, M. L., A potent lignan from Prunes alleviates inflammation and oxidative stress in lithium/pilocarpine-induced epileptic seizures in rats. *Antioxidants*, **2020**, *9*, 575, DOI: 10.3390/antiox9070575.

[9] Wallace, J. E.; Hamilton, H. E.; Shimek, E. L.; Schwertner, H. A.; Haegele, K. D., Determination of

phenylethylmalonamide by electron-capture gas chromatography. *Anal. Chem.* **1977**, *49*, 1969-1973, DOI: 10.1021/ac50021a021.

[10] Raithak, P. V.; Atkore, S. T.; Bondle, G. M., Identification of metabolites and evaluation of the seeds of Abrus precatorius (L.) by high resolution mass spectrometry. *Res. Sq*. **2021**, 1-10, DOI: 10.21203/rs.3.rs-146449/v1.

[11] Lafont, O.; Cave, C.; Menager, S.; Miocque, M., New chemical aspects of primidone metabolism. *Eur. J. Med. Chem.* **1990**, *25*, 61-66, DOI: 10.1016/0223-5234(90)90165-Y.

[12] Cooper, J. R.; Brodie, B. B., The enzymatic metabolism of hexobarbital (Evipal). *J. Pharmacol. Exp. Ther.* **1955**, *114*, 409-417.

[13] Calzetti, S.; Findley, L. J.; Pisani, F.; Richens, A., Phenylethylmalonamide in essential tremor. A double-blind controlled study. *J. Neurol. Neurosurg. Psychiatry*. **1981**, *44*, 932-934, DOI: 10.1136/jnnp.44.10.932.

[14] Streete, J. M.; Berry, D. J., Gas chromatographic analysis of phenylethylmalonamide in human plasma. *J. Chromatogr. B. Biomed. Sci. Appl.* 1987, *416*, 281-291, DOI: 10.1016/0378-4347(87)80511-X.

[15] Baumel, I. P.; Gallagher, B. B.; Mattson, R. H., Phenylethylmalonamide (PEMA): An important metabolite of primidone. *Arch. Neurol.* **1972**, *27*, 34-41, DOI: 10.1001/archneur.1972.00490130036005.

[16] Sanz-Prat, A.; Greskowiak, J.; Burke, V.; Villarreyes, C. A. R.; Krause, J.; Monninkhoff, B.; Sperlich, A.; Schimmelpfennig, S.; Duennbier, U.; Massmann, G., A model-based analysis of the reactive transport behaviour of 37 trace organic compounds during field-scale bank filtration. *Water. Res.* **2020**, *173*, 115523, DOI: 10.1016/j.watres.2020.115523.

[17] Kohn, W.; Sham, L. J., Self-consistent equations including exchange and correlation effects. *Phys. Rev.* **1965**, *140*, A1133-A1138, DOI: 10.1103/PhysRev.140.A1133.

[18] Becke, A. D., Density functional thermo chemistry – III: The role of exact exchange. *J. Chem. Phys.* **1993**, *98*, 5648-5652, DOI: 10.1063/1.464913.

[19] Lee, C.; Yang, W.; Parr, R. G., Development of the Colle-Salvetti correlation-energy formula into a functional of the electron density. *Phys. Rev. B.* **1988**, *37*, 785-789, DOI: 10.1103/PhysRevB.37.785.

[20] Frisch, M. J. *et al.,* Gaussion 09W, Revision A.02, Gaussion Inc. Walling ford, CT, **2009**.

[21] Zhurko, G A.; Zhurko, D A., Chemcraft Program Version 1.6 (Build 315), **2009**, http://www.chemcraftprog.com.

[22] Hehre, W. J.; Ditchfield, R.; Pople, J. A., Self-consistent molecular orbital methods. XII. Further extensions of gaussian-type basis sets for use in molecular orbital studies of organic molecules. *J. Chem. Phys.* **1972**, *56*, 2257-2261, DOI: 10.1063/1.1677527.

[23] Cheeseman, J. R.; Trucks, G. W.; Keith, T. A.; Frisch, M. J., A comparison of models for calculating nuclear magnetic resonance shielding tensors. *J. Chem. Phys.* **1996**, *104*, 5497-5509, DOI: 10.1063/1.471789.

[24] Petersilka, M.; Gossman, U. J.; Gross, E. K. U., Excitation energies from timedependent density-functional theory. *Phys. Rev. Lett.* **1966**, *76*, 1212-1215. DOI: 10.1103/PhysRevLett.76.1212.

[25] Runge, E.; Gross, E. K. U., Density functional theory for time-dependent systems, *Phys. Rev. Lett.* **1984**, *52*, 997. DOI: 10.1103/PhysRevLett.52.997.

[26] Thompson, M. A., ArgusLab 4.0.1 (Build 7600), **2004**, http://www.arguslab.com/.

[27] Sakamoto, J.; Nakagawa, T.; Kanehisa, N.; Kai, Y.; Katsura, M., 2-Phenylmalonamide, *Acta. Crystallogr. C.* **2000**, *56*, e485-e486, DOI: 10.1107/S0108270100011938.

[28] [28] Badawi, H. M., Molecular structure and vibrational assignments of 2, 4-dichlorophenoxyacetic acid herbicide. *Spectrochim. Acta A. Mol. Biomol. Spectrosc.* **2010**, *77*, 24-27, DOI: 10.1016/j.saa.2010.04.010.

[29] Fernandez, V. G.; Rajamannan, B.; Periandy, S.; Jayasheela, K., Quantum computational and spectral investigation of 4-chloro phenylacetyl chloride. *Gedrag Organ. Rev.* **2020**, *33*, 404-430.

[30] Dwivedi, C. P. D.; Sharma, S. N., Vibrational-spectra of 2-fluoro-4-bromo, 4-fluoro-2-bromo + 2-fluoro-5-bromo toluenes. *Indian J. Pure Appl. Phys.* **1973**, *11*, 446-447.

[31] Selvaraj, S.; Rajkumar, P.; Kesavan, M.;

Thirunavukkarasu, K.; Gunasekaran, S.; Saradha Devi, N.; Kumaresan, S., Spectroscopic and structural investigations on modafinil by FT-IR, FT-Raman, NMR, UV-Vis and DFT methods. *Spectrochim. Acta A. Mol. Biomol. Spectrosc.* **2020**, *224*, 117449, DOI: 10.1016/j.saa.2019.117449.

[32] Atac, A.; Caglar, K.; Gunnaz, S.; Karabacak, M., Vibrational (FT-IR and FT-Raman), electronic (UV-Vis), NMR (1H and 13C) spectra and reactivity analyses of 4,5-dimethyl-o-phenylenediamine. *Spectrochim. Acta A. Mol. Biomol. Spectrosc.* **2014**, *130*, 516-525, DOI: 10.1016/j.saa.2014.04.003.

[33] Thirunavukkarasu, K.; Rajkumar, P.; Selvaraj, S.; Suganya, R.; Kesavan, M.; Gunasekaran, S.; Kumaresan, S., Vibrational (FT-IR and FT-Raman), electronic (UV-Vis), NMR (1H and 13C) spectra and molecular docking analyses of anticancer molecule 4-hydroxy-3-methoxycinnamaldehyde. *J. Mol. Struct.* **2018**, *1173*, 307-320, DOI: 10.1016/j.molstruc.2018.07.003.

[34] Gunasekaran, S.; Kumaresan, S.; Arunbalaji, R.; Anand, G.; Seshadri, S.; Muthu, S., Vibrational assignments and electronic structure calculations for 6‐thioguanine. *J. Raman. Spectrosc.* **2009**, *40*, 1675-1681, DOI: 10.1002/jrs.2318.

[35] Seshadri, S.; Gunasekaran, S.; Muthu, S.; Kumaresan, S.; Arunbalaji, R., Vibrational spectroscopy investigation using *ab initio* and density functional theory on flucytosine. *J. Raman. Spectrosc.* **2007**, *38*, 1523-1531, DOI: 10.1002/jrs.1808.

[36] Ram Kumar, A.; Nithya, V.; Rajeshkumar, S.; Gunasekaran, S.; Kumaresan, S.; Selvaraj, S.; Selvam, K. A.; Devanathan, J., An experimental and theoretical evidence for structural and spectroscopic properties of 2-hydroxy-5-methoxybenzaldehyde. *The International Journal of Analytical and Experimental Modal Analysis*. **2019**, *9*, 1990-2003.

[37] Rajkumar, P.; Selvaraj, S.; Suganya, R.; Velmurugan, D.; Gunasekaran, S.; Kumaresan, S., Vibrational and electronic spectral analysis of thymol an isomer of carvacrol isolated from trachyspermum ammi seed: A combined experimental and theoretical study. *Chem. Data Collect.* **2018**, *15*, 10-31, DOI: 10.1016/j.cdc.2018.03.003.

[38] Premkumar, S.; Jawahar, A.; Mathavan, T.; Kumara Dhas, M.; Sathe, V. G.; Milton Franklin Benial, A., DFT calculation and vibrational spectroscopic studies of 2-(tert-butoxycarbonyl (Boc)-amino)-5-bromopyridin. *Spectrochim. Acta A. Mol. Biomol. Spectrosc.* **2014**, *129*, 74-83, DOI: 10.1016/j.saa.2014.02.147.

[39] Gunasekaran, S.; Arun Balaji, R.; Kumeresan, S.; Anand, G.; Srinivasan, S., Experimental and theoretical investigations of spectroscopic properties of N-acetyl-5-methoxytryptamine. *Can. J. Anal. Sci. Spect.* **2008**, *53*, 149-162.

[40] Selvaraj, S.; Rajkumar, P.; Kesavan, M.; Gunasekaran, S.; Kumaresan, S., Experimental and theoretical analyzes on structural and spectroscopic properties of monomer and dimeric form of (S)-Piperidine-2-Carboxylic acid: An attempt on medicinal plant. *Vib. Spectrosc.* **2019**, *100*, 30-39, DOI: 10.1016/j.vibspec.2018.10.008.

[41] Selvaraj, S.; Rajkumar, P.; Thirunavukkarasu, K.; Gunasekaran, S.; Kumaresan, S., Vibrational (FT-IR and FT-Raman), electronic (UV-Vis) and quantum chemical investigations on pyrogallol: A study on benzenetriol dimmers. *Vib. Spectrosc.* **2018**, *95*, 16-22, DOI: 10.1016/j.vibspec.2018.01.003.

[42] Selvaraj, S.; Rajkumar, P.; Santhiya, A.; Gunasekaran, S.; Kumaresan, S., 4-Methoxysalicylaldehyde: spectroscopic and computational investigations. *J. Emerg. Technol. Innov. Res*. **2018**, *5*, 222-229.

[43] Badertscher, M.; Buhlmann, P.; Pretsch, E., Structure Determination of Organic Compounds. Springer-Verlag Berlin Heidelberg, **2009**.

[44] Selvaraj, S.; Rajkumar, P.; Kesavan, M.; Gunasekaran, S.; Kumaresan, S.; Experimental and theoretical investigations on spectroscopic properties of tropicamide. *J. Mol. Struct.* **2018**, *1173*, 52-62, DOI: 10.1016/j.molstruc.2018.06.097.

[45] Aarthi, K. V.; Rajagopal, H.; Muthu, S.; Jayanthi, V.; Girija, R., Quantum chemical calculations, spectroscopic investigation and molecular docking analysis of 4-chloro-N-methylpyridine-2-carboxamide. *J. Mol. Struct.* **2020**, *1210*, 128053, DOI: 10.1016/j.molstruc.2020.128053.

[46] Varghese, H. T.; Panicker, C. Y.; Madhavan, V. S.;

Mathew, S.; Vinsova, J.; Alsenoy, C. V., FT-IR, FT-Raman and DFT calculations of the salicylanilide derivate 4-chloro-2-(-4-bromophenylcarbamoyl) phenylacetate. *J. Raman. Spectrosc.* **2009**, *40*, 1211-1223, DOI: 10.1002/jrs.2265.

[47] Ram Kumar, A.; Pavalarasu, L.; Kumaresan, S.; Selvaraj, S.; Devanathan, J.; Selvam, K. A., Structural analysis and confirmation of carbon atoms of gabapentin. *The International Journal of Analytical and Experimental Modal Analysis.* **2019**, *11*, 1315-1324.

[48] Selvaraj, S.; Rajkumar, P.; Kesavan, M.; Gunasekaran, S.; Kumaresan, S.; Rajasekar, R.; Renuga Devi, T. S., Spectroscopic and quantum chemical investigations on structural isomers of dihydroxybenzene. *J. Mol. Struct.* **2019**, *1196*, 291-305, DOI: 10.1016/j.molstruc.2019.06.075.

[49] Karabacak, M.; Kose, E.; Sas, E. B.; Kurt, M.; Asiri, A. M.; Atac, A., DFT calculations and experimental FT-IR, FT-Raman, NMR, UV-Vis spectral studies of 3-fluorophenylboronic acid. *Spectrochim. Acta A. Mol. Biomol. Spectrosc.* **2015**, *136*, 306-320, DOI: 10.1016/j.saa.2014.08.141.

[50] Ram Kumar, A.; Selvaraj, S.; Jayaprakash, K. S.; Gunasekaran, S.; Kumaresan, S.; Devanathan, J.; Selvam, K. A.; Ramadass, L.; Mani, M.; Rajkumar, P., Multi-spectroscopic (FT-IR, FT-Raman, ^{1}H NMR and ^{13}C NMR) investigations on syringaldehyde. *J. Mol. Struct.* **2021**, *1229*, 129490, DOI: 10.1016/j.molstruc.2020.129490.

[51] Thirunavukkarasu, K.; Rajkumar, P.; Selvaraj, S.; Gunasekaran, S.; Kumaresan, S., Electronic structure, vibrational (FT-IR and FT-Raman), UV-Vis and NMR analysis of 5-(4-(2-(5-ethylpyridin-2-yl) ethoxy) benzyl) thiazolidine-2,4-dione by quantum chemical method. *Chem. Data Collect.* **2018**, *17*, 263-275, DOI: 10.1016/j.cdc.2018.09.006.

[52] Foster, A. J.; Weinhold, F., Natural hybrid orbitals. *J. Am. Chem. Soc.* **1980**, *102*, DOI: 10.1021/ja00544a007.

[53] Reed, A. E.; Weinstock, R. B.; Weinhold, F., Natural population analysis. *J. Chem. Phys.* **1985**, *83*, 735-746, DOI: 10.1063/1.449486.

[54] Reed, A. E.; Weinhold, F., Natural localized molecular orbitals. *J. Chem. Phys.* **1985**, *83*, 1736-1740, DOI: 10.1063/1.449360

[55] Reed, A. E.; Curtiss, L. A.; Weinhold, F., Intermolecular interactions from a natural bond orbital, donor-acceptor viewpoint. *Chem. Rev.* **1988**, *88*, 899-926, DOI: 10.1021/cr00088a005.

[56] Uludag, N.; Serdaroglu, G., A DFT investigation on the structure, spectroscopy (FT-IR and NMR), donor-acceptor interactions and non-linear optic properties of (±)-1,2-dehydroaspidospermidine. *Chem. Select*, **2019**, *4*, 6870-6878, DOI: 10.1002/slct.201901383.

[57] Serdaroglu, G., Harmine derivatives: a comprehensive quantum chemical investigation of the structural, electronic (FMO, NBO, and MEP), and spectroscopic (FT-IR and UV-Vis) properties. *Res. Chem. Intermediat.* **2020**, *46*, 961-982, DOI: 10.1007/s11164-019-04020-x.

[58] Serdaroglu, G.; Uludag, N., The electronic and spectroscopic investigation of (±)-dasycarpidone. *Vib. Spectrosc.* **2020**, *111*, 103156, DOI: 10.1016/j.vibspec.2020.103156.

[59] [59] Mary, Y. S.; Mary, Y. S.; Serdaroglu, G.; Sarojini, B. K., Conformational analysis and quantum descriptors of two bifonazole derivatives of immense anti-tuber potential by using vibrational spectroscopy and molecular docking studies. *Struct. Chem.* **2021**, *32*, 859-867, DOI: 10.1007/s11224-020-01678-7.

[60] Al-Otaibi, J. S.; Mary, Y. S.; Mary, Y. S.; Serdaroglu, G., Adsorption of adipic acid in Al/BN/P nanocages: DFT investigations. *J. Mol. Modeling.* **2021**, *27*, 1-7, DOI: 10.1007/s00894-021-04742-z.

[61] Mahalakshmi, G.; Balachandran, V., NBO, HOMO, LUMO analysis and vibrational spectra (FTIR and FT Raman) of 1-amino 4-methylpiperazine using *ab initio* HF and DFT methods. *Spectrochim. Acta A. Mol. Biomol. Spectrosc.* **2015**, *135*, 321-334, DOI: 10.1016/j.saa.2014.06.157.